Assessment of cerebral autoregulation in patients undergoing anaesthesia with propofol: a comparison among spontaneous variability methods

Roberta Saputo[1], Laura Sparacino[1], Riccardo Pernice[1], Francesca Gelpi[2], Vlasta Bari[2,3], Alberto Porta[2,3], Luca Faes[1]

[1] *Department of Engineering, University of Palermo, Viale delle Scienze, Building 9, 90128 Palermo, Italy*
[2] *Department of Biomedical Sciences for Health, University of Milan, 20133 Milan, Italy*
[3] *Department of Cardiothoracic, Vascular Anesthesia and Intensive Care, IRCCS Policlinico San Donato, 20097 San Donato Milanese, Italy*

***Abstract*— Cerebral autoregulation (CA) is a fundamental homeostatic mechanism that maintains cerebral blood flow (CBF) within a constant range despite blood pressure variations. In this work, two different approaches for assessing CA are compared, i.e. the autoregulation index (ARI) and dynamic entropy measures. The arterial pressure and the CBF velocity were acquired on eighteen subjects undergoing coronary artery bypass graft surgery, before induction of general anaesthesia with propofol and during anaesthesia. The ARI-based method confirmed the known result that CA remains unchanged with propofol. Entropy measures led to complementary findings, suggesting an increased dependence of cerebral blood flow dynamics on systemic pressure, probably due to the effect of mechanical breathing during surgery.**

***Keywords*—Cerebrovascular autoregulation, autoregulation index, entropy, linear parametric autoregressive modelling.**

I. Introduction

Cerebrovascular autoregulation (CA) is a critical process in humans for maintaining adequate cerebral blood flow (CBF) values in response to external or internal system disturbances, such as changes in arterial blood pressure (AP) [1]. The assessment of CA can be carried out by measuring changes in CBF in response to slow (static method) [2] or rapid changes (dynamic method) [3] in AP. While the static method requires external invasive intervention to induce changes in AP, the use of the transcranial Doppler ultrasound technique (TCD) allow the non-invasive assessment of dynamic CA through the investigation of the beat-to-beat CBF changes in relation to AP changes occurring spontaneously [4], under the assumption that CBF velocity is approximately equal to CBF [3]. Indeed, the non-invasive characterization of CA is based on the study of the dynamic closed-loop interactions between the mean AP (MAP) and the mean CBF velocity (MCBFV) along the pressure-to-flow link of the closed-loop system, i.e. considering the interactions directed from MAP to MCBFV. CA is defined as the intrinsic control mechanism operating along this reflex and aiming to maintain a constant and stable MCBFV despite beat-to-beat variations of MAP, while preserving some degree of uncoupling between MCBFV and MAP over a range of values of MAP as wide as possible [4]–[6]. Dynamic CA has been evaluated exploiting different methods, such as the MAP-MCBFV closed-loop system transfer function [7], the autoregulation index (ARI) [4], [8], and linear parametric autoregressive models [9], [10]. In particular, the ARI index models the response of MCBFV to changes in MAP by a system of differential equations in which each estimated MCBFV curve, numbered from 0 to 9, represents a different level of CA [4]. The computation of ARI can be carried out by considering three different approaches, i.e. the time domain method (TDM) [11] , the non-parametric method (non-PM) [12] and the parametric method (PM) [9]. Recently, measures of dynamic entropy for bivariate systems [13] have been developed, which are derived from full and restricted autoregressive models and can be exploited to study the dynamic interactions along the pressure-to-flow link.

The present study focuses on the assessment of dynamic CA in patients scheduled for coronary artery bypass graft (CABG) surgery, before and during general anaesthesia with propofol [14]. Two different approaches are exploited to investigate CA mechanisms, i.e. the ARI and measures of dynamic entropy for bivariate systems [13]. Herein, we use the PM to assess CA, consistently with entropy measures which are also based on linear parametric modelling of time series under the hypothesis of Gaussian processes [13], [15]. The parametric ARI and entropy-based measures are compared evaluating their degree of correlation, with the aim to evidence whether the two investigated methods highlight similar or different aspects of cerebrovascular physiology, also allowing to better understand the role of confounding factors in the closed-loop interactions between CBF and AP.

II. Materials and Methods

A. Experimental protocol and series extraction

Eighteen patients (age: 63.8 ± 7.8 yrs, 1 female) scheduled for CABG surgery were enrolled at the Department of Cardiothoracic, Vascular Anaesthesia and Intensive Care of IRCCS Policlinico San Donato, San Donato Milanese, Milan, Italy [14]. Patients signed an informed consent before participating to the study and were examined ahead of surgery before induction of general anaesthesia (PRE) and after intubation of the trachea, during general anaesthesia, before opening the chest (POST). During the PRE session, subjects were breathing spontaneously, whereas during the POST session they were mechanically ventilated with a rate of 12-16 breaths/min. The PRE session was recorded after application of standard premedications including intramuscular administration of atropine (0.5 mg) and fentanyl (100 μg). Anaesthesia was induced by the intravenous bolus injection of propofol and remifentanil. The POST session was recorded when the target plasma concentration of propofol was expected to be around 3 μg/ml based the pharmacokinetic properties of the drug.

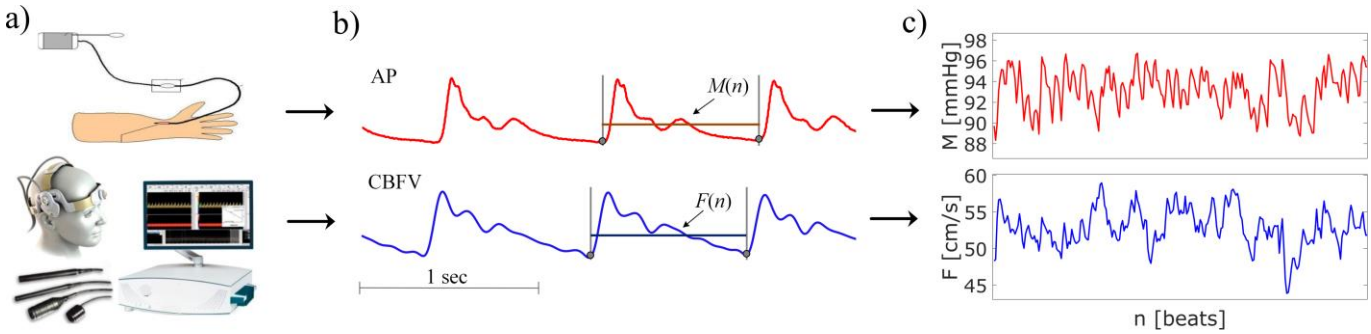

Fig. 1 (a) Schematic representation of the biomedical instrumentation used for data acquisition: (top) invasive measurement of AP by a catheter inserted into the radial artery; (bottom) transcranial Doppler ultrasound (TCD) device with ultrasound probes and adjustable helmet for CBFV acquisition from the middle cerebral artery (right or left). **(b)** exemplary traces of the acquired AP and CBFV signals for a representative subject; **(c)** the M and F time series are extracted respectively by integrating the AP signal within the diastolic pulse interval and the CBFV signal between its two minima within the cardiac period.

Electrocardiogram (ECG, lead II), invasive AP from the radial artery and CBF velocity (CBFV) from the middle cerebral arteries through a TCD device were simultaneously acquired. The acquisition phase in PRE and POST conditions lasted about 6 minutes. After signal acquisition, MAP and MCBFV stationary time series of 250 beats each were extracted by integrating respectively the AP and CBFV signals between two consecutive diastolic points and dividing by the time interval between them. In the following, we refer to MAP and MCBFV time series as M and F, respectively. Further details about the experimental protocol, signal acquisition and series extraction can be found in [14]. The schematic representation of the acquisition system, a representative example of the acquired signals and the extracted time series are shown in Fig. 1.

B. Autoregulation Index (ARI): parametric estimation

The autoregulation index (ARI) allows to assess CA by modelling F through a system of ten ordinary differential equations in agreement with the derivative filter model originally introduced by Tiecks et al. [4]. The Tiecks' model provides a set of ten step responses, in which each predicted F curve ranks the efficiency of CA from 0, i.e. absent CA, to 9, i.e. excellent CA, with ARI values lower than or equal to 4 indicating impaired CA [4]. The ten F curves derived from this model are compared with the F curve estimated from the parametric linear representation of the dynamic F-M relationship. More precisely, an auto and cross regressive model (ARX) is applied to describe the dynamical evolution of F due to beat-to-beat changes of both F and M [8]. After the application of a linear detrending to both series, the sample F_k, where k is the current time instant, is described as the linear combination of p past values of F weighted by the coefficients a_i, with $i = 1,\dots,p$, plus the linear combination of $p - \tau + 1$ past values of M weighted by the coefficients b_i, with $i = \tau,\dots,p$, plus a random unpredictable portion W_k being the sampling of a Gaussian white noise W with zero mean and variance λ^2:

$$F_k = \sum_{i=1}^{p} a_i F_{k-i} + \sum_{i=\tau}^{p} b_i M_{k-i} + W_k, \qquad (1)$$

where p is the model order and τ is the lag of the faster interactions from M to F. By representing the model coefficients in the Z domain as $A(z) = \sum_{i=1}^{p} a_i z^{-i}$ and $B(z) = \sum_{i=\tau}^{p} b_i z^{-i}$, the transfer function from M to F, which provides the coefficients of the impulse response, can be written as:

$$H_{F-M}(z) = \frac{B(z)}{1-A(z)}. \qquad (2)$$

The impulse response was truncated to 31 values taking the cardiac beats from 0 to 30. After integrating the impulse response to obtain the step response, the comparison between each of the ten step responses derived from the Tiecks' model and the data-driven step response was carried out via the normalized mean square prediction error (NMSPE), computed as the mean square value of the difference between the measured and the predicted F curves normalized by the mean square value of the measured F curve [8]. We selected the optimal ARI (i.e. from 0 to 9) as the value corresponding to the minimum value of NMSPE. Further details on the proposed method can be found in [8].

C. Dynamic information measures

Given the bivariate process S = {M, F}, where M is the driver and F is the target process, the framework of information theory allows the study of the dynamic interactions along the pressure-to-flow link by quantifying the information content of the target in terms of predictive information $P_{F|S}$ (i.e., information contained in the target that can be described by the past history of the entire process S). Using the chain rule, $P_{F|S}$ can be decomposed in two different ways [13]:

$$\text{(i)} P_{F|S} = S_F + T_{M\to F};\ \text{(ii)}\ P_{F|S} = C_{M\to F} + S_{F|M}, \qquad (3)$$

where S_F is the self-entropy (information carried by the present state of the target that can be predicted by its own past), $T_{M\to F}$ is the transfer entropy (information carried by the present of the target that can be predicted by the past of the driver above and beyond the part that is predicted by the past of the target), $C_{M\to F}$ is the cross-entropy (information carried by the present state of the target that can be predicted exclusively by the past of the driver), $S_{F|M}$ is the conditional self-entropy (information carried by the present state of the target that can be predicted by its past above and beyond the part that is predicted by the past of the driver) [13]. Under the assumption of joint gaussianity of the observed bivariate process [15], the dynamic information measures introduced above were evaluated using model-based estimators as:

$$S_F = \frac{1}{2} ln \frac{\sigma_F^2}{\sigma_{AR}^2};\ T_{M\to F} = \frac{1}{2} ln \frac{\sigma_{AR}^2}{\sigma_{ARX}^2} \qquad (4)$$

$$C_{M\to F} = \frac{1}{2} ln \frac{\sigma_F^2}{\sigma_X^2};\ S_{F|M} = \frac{1}{2} ln \frac{\sigma_X^2}{\sigma_{ARX}^2} \quad (5)$$

where σ_F^2 is the variance of the target process, σ_{AR}^2 is the prediction error variance of an auto-regressive (AR) model describing the present state of the target from its past values, σ_X^2 is the prediction error variance of a cross-regressive (X) model describing the present state of the target from the past values of the driver, σ_{ARX}^2 is the prediction error variance of an ARX model describing the present state of the target from the past values of the entire bivariate process. The computation of the dynamic information measures in (4) and (5) thus reduces to the estimation of the error variances of full (ARX) and restricted (AR, X) linear regression models, which was performed by solving the Yule-Walker equations [13].

D. Data pre-processing

The acquired M and F time series were first pre-processed to obtain zero-mean series. As regards the computation of the dynamic entropy measures, further pre-processing was performed using an AR high-pass filter for detrending (zero-phase filter, cut-off frequency of 0.0156 times the sampling frequency, the latter assumed to be the inverse of the mean HP for each subject); model identification was performed by setting the model order according to the Akaike Information Criterion (AIC) for each subject (with maximum scanned model order equal to 14). As regards the parametric ARI computation, the model order was set in accordance with [16].

E. Statistical and correlation analysis

The significance of the differences between experimental conditions (PRE vs. POST) was assessed using non-parametric tests, given the small sample size and that normality of the series assessed through Anderson-Darling test was rejected for most cases. Specifically, the paired Wilcoxon signed rank test was used with a significance level of 5%.

Moreover, the non-parametric Spearman correlation coefficient, corresponding to Pearson correlation coefficient computed from rank vectors [17] was used to assess the degree of correlation between the parametric ARI and the entropy-based linear measures. Indeed, given its non-parametric nature, the assumption of Gaussianity is not a necessary condition and thus it is used to compare discrete variables, such as the ARI, with continuous variables, such as the measures of dynamic entropy. In this study, the parametric ARI values were compared with each of the entropy measures (self-entropy, transfer entropy, cross entropy, and conditional self-entropy) for any given experimental condition.

III. RESULTS AND DISCUSSION

Figure 2 shows the distributions across subjects of ARI values obtained with the parametric method (Fig. 2a), transfer entropy and self-entropy (Fig. 2b, c), cross entropy and conditional self-entropy (Fig. 2d, e), evaluated in the PRE and POST experimental conditions. The ARI method evidenced that CA remained intact during the PRE-POST protocol (Fig. 2a), confirming that propofol general anaesthesia does not affect CA [16]. In fact, although propofol general anaesthesia is known to cause autonomic depression, which is a major determinant of CA [18], several studies exploiting the same experimental protocol have confirmed that CA does not vary with the anaesthetic pharmacokinetic properties of propofol [16].

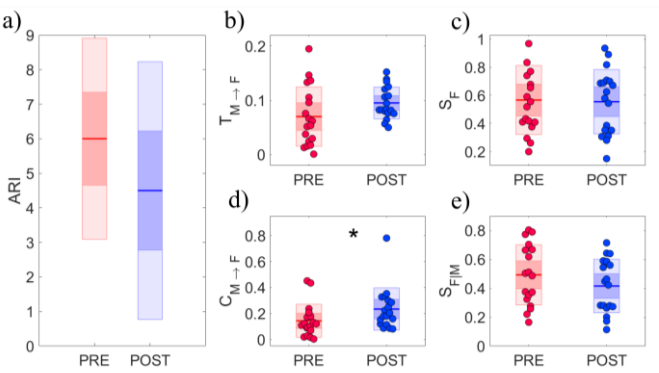

Fig. 2 Results of short-term cerebrovascular variability analysis. Boxplots depict the distributions of **(a)** ARI values computed with the parametric method, **(b)** transfer entropy $T_{M\to F}$, **(c)** self-entropy S_F, **(d)** cross entropy $C_{M\to F}$ and **(e)** conditional self-entropy $S_{F|M}$ in PRE (left boxplots, red dots) and POST (right boxplots, blue dots) conditions. Statistically significant differences (p<0.05): *****, PRE vs POST, Wilcoxon signed rank test for paired data.

Measures of dynamic entropy show different interpretations of how predictable dynamics in the target process are derived from its own past and the past of the driver process. The increased cross-entropy in POST (Fig. 2d, $p = 0.0386$) reflects a higher predictability of CBFV dynamics from AP values, documenting an increased cerebrovascular coupling that might be indicative of reduced cerebral autoregulation (CBFV changes are more dependent on AP variations). However, the finding that $T_{M\to F}$ and $S_{F|M}$ do not vary between conditions (Fig. 2b, c) leads us to suggest that the causal interactions from M to F and the internal dynamics of F may be unaffected by the investigated experimental protocol. Since variations in the cross-entropy can be induced by changes in the direct coupling along both directions of interaction (M→F and F→M in this case) [13], caution should be used in ascribing to a stronger coupling the increased cross-predictability of F given M. Moreover, the simultaneous effect induced by mechanical breathing on M and F during anaesthesia in POST, although not directly investigated, could have generated regular oscillations in both series at the frequency of mechanical ventilation. This would have caused an increased predictability of F from M, which appears when considering $C_{M\to F}$ but not $T_{M\to F}$, i.e. when conditioning also on the past dynamics of F apart from M [19].

Table 1 reports the correlation values between the ARI and each of the dynamic entropy measures, evaluated with the Spearman correlation index (ρ) in the PRE-POST protocol. The weak correlations, confirmed by p values higher than the significance threshold (level of significance of 5%), suggest that ARI and dynamic entropy measures provide different information on the short-term cerebrovascular control and on the functioning of CA in this group of patients.

IV. CONCLUSION

This work aimed to compare different methods for investigating the interaction link from arterial blood pressure to cerebral blood flow (i.e., the pressure-to-flow link), to investigate the physiological mechanisms related to cerebral

autoregulation. The ARI-based method showed that CA remained unchanged with the PRE-POST protocol in patients undergoing CABG surgery, confirming the known properties of propofol on CA maintenance. On the other hand, the statistically significant increase of cross-entropy after the induction of general anaesthesia showed that the dynamics of cerebral blood flow become more dependent on those of systemic pressure, suggesting a possible alteration of cerebral autoregulatory mechanisms. The weak correlation between the two methods confirms that they highlight different aspects of cerebrovascular physiology.

To corroborate the results of this work, future studies should be designed: (i) to investigate cerebrovascular interactions through a closed-loop analysis considering also the effects of cerebral flow variations on arterial pressure; and (ii) to quantify such interactions in the frequency domain separating respiration-related oscillations from effects within the very low frequency (0.02-0.07 Hz) and low frequency (0.07-0.2 Hz) bands during the PRE-POST protocol [6].

TABLE I
SPEARMAN CORRELATION: ARI VS. ENTROPY MEASURES

	PRE		*POST*	
	ρ	*p-value*	*ρ*	*p-value*
ARI vs $T_{M\to F}$	-0.012	0.961	0.447	0.063
ARI vs $C_{M\to F}$	-0.327	0.185	0.254	0.308
ARI vs S_F	-0.224	0.372	0.008	0.974
ARI vs $S_{F\|M}$	-0.012	0.423	-0.114	0.654

Comparison between parametric ARI and dynamic information measures (transfer entropy $T_{M\to F}$, self entropy S_F, cross entropy $C_{M\to F,}$ conditional self entropy $S_{F|M}$) using Spearman correlation index ρ during the PRE and POST experimental conditions. Rejection of the null hypothesis (*p*-value < 0.05) means that the two investigated metrics are significantly correlated.

ACKNOLEDGMENT

This work was supported by "Sensoristica intelligente, infrastrutture e modelli gestionali per la sicurezza di soggetti fragili" (4FRAILTY) project, funded by Italian MIUR (PON R&I 2014-20, grant no. ARS01_00345). R.P. is partially supported by European Social Fund (ESF) Complementary Operational Programme (POC) 2014/2020 of the Sicily Region.

REFERENCE

[1] N. A. Lassen, "Cerebral blood flow and oxygen consumption in man," *Physiol Rev*, vol. 39, no. 2, pp. 183–238, 1959.
[2] O. B. Paulson, S. Strandgaard, and L. Edvinsson, "Cerebral autoregulation.," *Cerebrovasc Brain Metab Rev*, vol. 2, no. 2, pp. 161–192, 1990.
[3] D. W. Newell, R. Aaslid, A. Lam, T. S. Mayberg, and H. R. Winn, "Comparison of flow and velocity during dynamic autoregulation testing in humans.," *Stroke*, vol. 25, no. 4, pp. 793–797, 1994.
[4] F. P. Tiecks, A. M. Lam, R. Aaslid, and D. W. Newell, "Comparison of static and dynamic cerebral autoregulation measurements," *Stroke*, vol. 26, no. 6, pp. 1014–1019, 1995.
[5] R. Aaslid, K.-F. Lindegaard, W. Sorteberg, and H. Nornes, "Cerebral autoregulation dynamics in humans.," *Stroke*, vol. 20, no. 1, pp. 45–52, 1989.
[6] J. A. H. R. Claassen, A. S. S. Meel-van den Abeelen, D. M. Simpson, R. B. Panerai, and I. C. A. R. N. (CARNet), "Transfer function analysis of dynamic cerebral autoregulation: A white paper from the International Cerebral Autoregulation Research Network," *Journal of Cerebral Blood Flow & Metabolism*, vol. 36, no. 4, pp. 665–680, 2016.
[7] R. Zhang, J. H. Zuckerman, C. A. Giller, B. D. Levine, J. H. Zuckerman, and C. A. Giller, "Transfer function analysis of dynamic cerebral autoregulation in humans," *American Journal of Physiology-Heart and Circulatory Physiology*, vol. 274, no. 1, pp. H233--H241, 1998.
[8] F. Gelpi *et al.*, "Dynamic cerebrovascular autoregulation in patients prone to postural syncope: comparison of techniques assessing the autoregulation index from spontaneous variability series," *Autonomic Neuroscience*, vol. 237, p. 102920, 2022.
[9] R. B. Panerai, S. L. Dawson, and J. F. Potter, "Linear and nonlinear analysis of human dynamic cerebral autoregulation," *American Journal of Physiology-Heart and Circulatory Physiology*, vol. 277, no. 3, pp. H1089–H1099, 1999.
[10] R. Pernice *et al.*, "Spectral decomposition of cerebrovascular and cardiovascular interactions in patients prone to postural syncope and healthy controls," *Autonomic Neuroscience*, vol. 242, p. 103021, Nov. 2022, doi: 10.1016/j.autneu.2022.103021.
[11] R. B. Panerai, P. J. Eames, and J. F. Potter, "Variability of time-domain indices of dynamic cerebral autoregulation," *Physiol Meas*, vol. 24, no. 2, p. 367, 2003.
[12] R. B. Panerai, R. P. White, H. S. Markus, and D. H. Evans, "Grading of cerebral dynamic autoregulation from spontaneous fluctuations in arterial blood pressure," *Stroke*, vol. 29, no. 11, pp. 2341–2346, 1998.
[13] L. Faes, A. Porta, and G. Nollo, "Information decomposition in bivariate systems: theory and application to cardiorespiratory dynamics," *Entropy*, vol. 17, no. 1, pp. 277–303, 2015.
[14] A. Porta, V. Bari, T. Bassani, A. Marchi, V. Pistuddi, and M. Ranucci, "Model-based causal closed-loop approach to the estimate of baroreflex sensitivity during propofol anesthesia in patients undergoing coronary artery bypass graft," *J Appl Physiol*, vol. 115, no. 7, pp. 1032–1042, 2013.
[15] L. Barnett, A. B. Barrett, and A. K. Seth, "Granger causality and transfer entropy are equivalent for Gaussian variables," *Phys Rev Lett*, vol. 103, no. 23, p. 238701, 2009.
[16] V. Bari *et al.*, "Exploring metrics for the characterization of the cerebral autoregulation during head-up tilt and propofol general anesthesia," *Autonomic Neuroscience*, p. 103011, 2022.
[17] S. Kim, M. Ouyang, and X. Zhang, "Compute spearman correlation coefficient with Matlab/CUDA," in *2012 IEEE international symposium on signal processing and information technology (ISSPIT)*, 2012, pp. 55–60.
[18] F. Boer, P. Ros, J. G. Bovill, P. van Brummelen, and J. van der Krogt, "Effect of propofol on peripheral vascular resistance during cardiopulmonary bypass," *Br J Anaesth*, vol. 65, no. 2, pp. 184–189, 1990.
[19] A. Porta *et al.*, "Categorizing the Role of Respiration in Cardiovascular and Cerebrovascular Variability Interactions," *IEEE Trans Biomed Eng*, vol. 69, no. 6, pp. 2065–2076, 2021.